Journal Name

Dynamic Article Links ►

Cite this: DOI: 10.1039/c0xx00000x

www.rsc.org/xxxxxx

ARTICLE TYPE

Facile and Green fabrication of Multiple Magnetite Nano-cores @Void@Porous Shell Microspheres for Delivery Vehicles

Lei Bi, Gang Pan*

Received (in XXX, XXX) Xth XXXXXXXXX 20XX, Accepted Xth XXXXXXXXX 20XX

DOI: 10.1039/b000000x

Multiple magnetite nano-cores@void@porous shell microspheres have been fabricated by using the algae cell wall as the hollow porous shell precursor and the intracellular substances as the reducing agents to form magnetite cores inside the microspheres via hydrothermal reactions. This method not only simplified the fabricating steps and superseded harmful chemical reagents, but also endow the microspheres with a uniform size (~2.5 um), porous shell (~15 nm), multiple magnetite nano-cores (~25 nm) and high void volume ratio (> 70%). The product presents fast magnetic separation and redispersibility as well as pH-switched protein auto-loading (high capacity > 600 mg g^{-1}) and unloading as high performance deliver vehicles.

The synthesis of the magnetic core@void@shell rattle type[1] (or so called yolk-shell[2]) micro/nano spheres (MCRSs) have stimulated great interest not only for their appealing structures but also for many technological applications, including: microwave adsorption, catalysis, magnetically-triggered drug release and so on.[3] These promising applications profit from the novel structure of a magnetically responsive core, functional shell[4] and void space for loading guest materials[5]. Recently, many attentions have been received on the fabrication of MCRSs using selective etching or dissolution, soft template, Ostwald ripening and ship in bottle methods.[6] These methods are primarily based on the pre-core/post-shell or pre-shell/post-shell strategy.[7]

In spite of the success of these works in fabricating MCRSs, there are still some difficult problems that need to be solved. For instance, 1) most of these MCRSs have only one big magnetic core, which left limited space in the cavity. Actually, multiple small cores in sufficient void space (high volume ratio) are more advantageous than one big core in limited void space[8], because multiple small cores can improve the physical and chemical interactions between the particles and the target objects by adding more reactive sites, furthermore, sufficient void space can be used to load more guest materials. However, it is still a challenge to prepare rattle type microspheres with multiple magnetic cores and high void volume ratio. 2) in order to fabricate complex core@void@shell configuration, tedious procedures, harsh reaction conditions, and environmental harmful chemicals are often inevitable, which not only limited the advanced function of the material but also make the practical production and application of these materials problematic. These limitations can hardly be lifted without the breakthrough in the existing pre-core/post-shell and pre-shell/post-shell strategies.

Chlorella pyrenoidosa, as an inexpensive, abundant, and renewable native biomaterial resource, has been used to produce biofuel[9] and named as a green healthy food by FAO[10]. The cell wall of Chlorella pyrenoidosa is constructed primarily of α-cellulose and hemicellulose, which provide physical protection for the whole cell system[11]. The direct use of the cell wall as the shell precursor may effectively simplify the synthetic step of rattle type microspheres. Some biological extracts have been used as natural reagents for fabrication of magnetic nanoparticles[12]. However, these biological extracts require toxic chemical solvent and complicated extraction processes, direct use of native biomaterial may circumvents these problems[13]. Therefore, we conjecture that the rich intracellular substances of the Chlorella pyrenoidosa may supersede harmful chemical reagents for the formation of the internal nanocores.

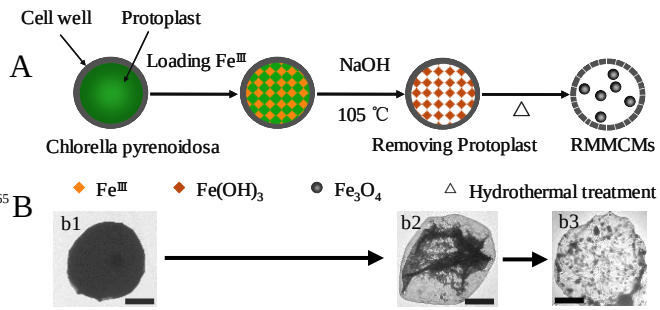

Scheme 1. (A) The fabrication processes for the RMMCMs. (B) The TEM images of the RMMCMs in each step: (b1) Chlorella pyrenoidosa cell, (b2) the cell wall of Chlorella pyrenoidosa with iron hydroxide, (b3) the RMMCMs obtained by the hydrothermal treatment at 200°C for 4 h. All scale bars are 1 um.

In this work, we propose a novel method for fabricating rattle-type multiple magnetite cores microspheres with porous biopolymer shell (RMMCMs) through mild hydrothermal method (200°C). Only three cheap raw materials, i.e. environmentally friendly Chlorella pyrenoidosa cells, ammonium iron citrate, and sodium hydroxide, were used to synthesize the RMMCMs products. The preparing procedure of RMMCMs is illustrated in Scheme 1. Firstly, iron precursor (Fe^{III}) was loaded by dispersing the Chlorella pyrenoidosa powder in the solution of ferric ammonium citrate for 12 h and then washed off the excess of the iron precursor solution with pure water. Next, the protoplast

inside the Chlorella pyrenoidosa cells was removed by hot (105°C) NaOH solution (6%) to get the hollow shell, meanwhile the iron hydroxide of low solubility was formed inside the hollow shell. Finally, the magnetite nano-cores and the porous shell were formed simultaneously by the hydrothermal treatment at 200°C for 4 h. The formation process of the RMMCMs could be observed from the TEM images in Scheme 1 (B). The morphology change from spherical Chlorella pyrenoidosa cell (Scheme 1 B (b1)) to hollow shell (Scheme 1 B (b2)) may be due to the fact that protoplast inside the Chlorella pyrenoidosa could be dissolved in hot NaOH solution but not the cell wall [11]. After hydrothermal treatment, the final product of RMMCMs (Scheme 1B(b3)) was obtained.

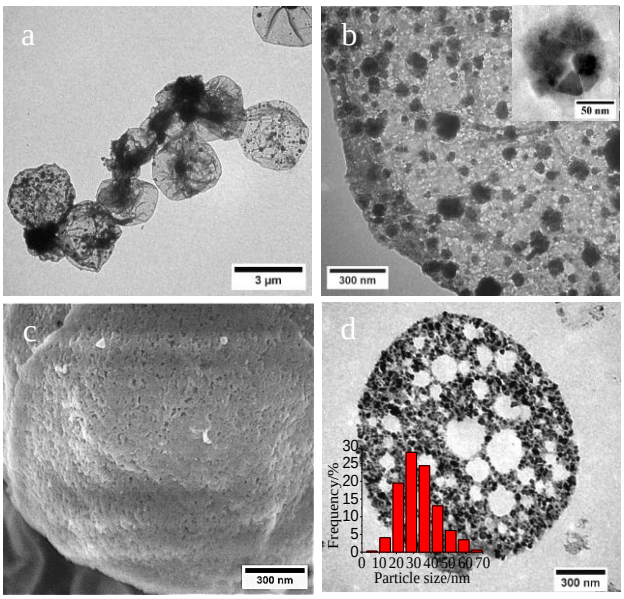

Figure 1. a) and b) TEM images of RMMCMs; the inset in b) is a FETEM image of the particles inside the RMMCMs; c) FESEM image of RMMCMs; d) TEM image of ultramicrotomed a single RMMCMs; the inset in d) is the size distribution of the particles inside the RMMCMs.

The TEM image in Figure 1a shows that the microspheres preserve as integral hollow spherical (~2.5 um) embedded with multiple particles (~100 nm) with void spaces among the particles and the shell. The void volume ratio of the particles and the void space in the microspheres is about 1:3. The shell thickness is about 40 nm (Figure 1a) and there are some pores in the shells (Figure 1b). Field emission scanning electron microscopy (FESEM) image further confirms the existence of the pores in the shell (Figure 1c). The N_2 adsorption-desorption isotherm of RMMCMs displayed a hysteresis loop, which is characteristics of mesoporous material. Data calculated using the BJH (Barrett-Joyner-Halenda) method reveals that the average size of the shell pores was about 15 nm (Figure S1, Supporting Information). The BET surface area of RMMCMs was 64.1 $m^2 g^{-1}$. The formation of pores may be due to the differences in the hydrolysis resistance of different components in the cell wall[14]. FETEM (inset in Figure 1b) examination of the particles suggests that these micro particles were made up of several nanoparticles. In order to obtain the actual distribution of the particles and the structures inside the RMMCMs, the microspheres were embedded with epoxy resins and ultramicrotomed into thin slices and analyzed with TEM. Most of the nanoparticles are in the range 20 nm to 40 nm (inset in Figure 1d) and localized inside the microspheres where many cavities are also observed. In comparison, only few nanoparticles were found on the exterior surface of the microspheres (Figure 1c). Since the particle size is larger than the apertures of the shell, these nanoparticles and their clusters can be well confined inside the microspheres.

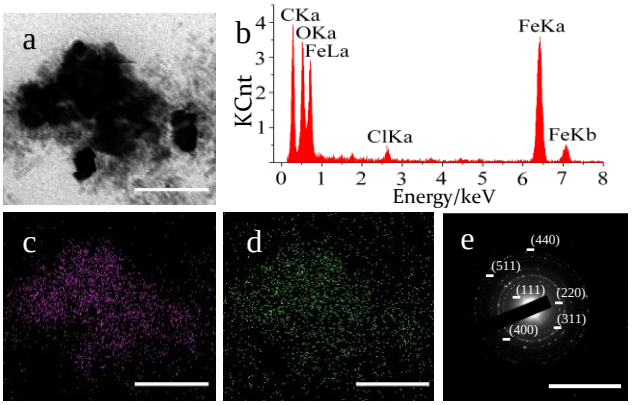

Figure 2. a), b), c) and d) FETEM image, EDX spectrum, Elemental maps of Fe and O and SAED pattern of the nanoparticles inside the RMMCMs, respectively. All scale bars are 100 nm.

In order to identify the structure and composition of the nanoparticles inside the RMMCMs, energy-dispersive X-ray (EDX) spectrum, elemental mapping characterization and selected-area electron diffraction (SAED) were carried out by using JEM 2100F field emission transmission electron microscope. Figure 2a displays the normal FETEM image of the nanoparticles inside the RMMCMs. Peaks of C, O, Fe and Cl are identified from the EDX spectrum (Figure 2b). The C and Cl peaks can be attributed to epoxy resin and hydrochloric acid that are used in the sample treatment. The Fe and O peaks can only be assigned to the nanoparticles (Figure 2c, 2d). In Figure 2e, the SAED pattern contains at least six well-defined spotted rings, the spotted appearance of the diffraction rings is due to high crystallinity of the obtained nanoparticles[15]. The corresponding lattice spacing calculated from the SAED pattern (Table S1, Supporting Information) are consistent with the standard magnetite (JCPDS no. 99-0073).

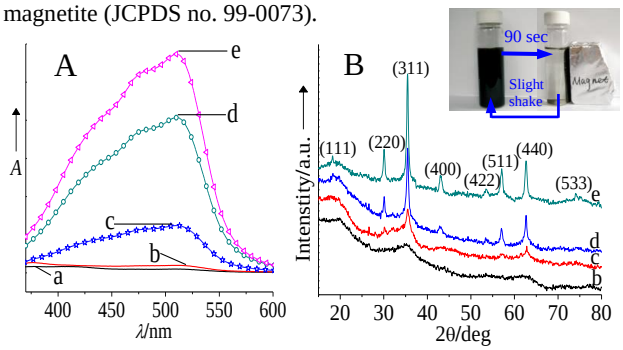

Figure 3. UV/Vis spectra (A) of Fe^{II}-phen acid solutions obtained by adding 1, 10-phenanthroline in the acid extract of the powder samples (a-e). XRD patterns (B) of the powder samples (b-e). (a) Chlorella pyrenoidosa containing Fe^{III}; (b) obtained by removing the protoplast of sample (a) under hot (105°C) NaOH solution(6%); (c), (d) and (e) were prepared by hydrothermal treatment of sample (b) under 170°C, 185°C and 200°C, respectively. The inset pictures in (B) show that the RMMCMs (200°C) possess fine magnetic responsivity and redispersibility.

During the synthesis procedures of RMMCMs, Fe^{III} was used as the single iron precursor, but the magnetite contains both Fe^{II} and Fe^{III}.[16] It is necessary to confirm whether Fe^{II} exist in the RMMCMs products. Fe^{II} salts in acidic solutions react with 1, 10-phenanthroline to form a dark red complex (Fe^{II}-phen), and the maximum absorption wave length of this complex is 510 nm. Fe^{III} salts do not react under these conditions[16]. The UV-vis spectra were used to identify the existence of the Fe^{II}-phen compound. XRD was used to research the phase transition of RMMCMs under different reaction temperatures. Figure 3A(a) shows that, after loading Chlorella pyrenoidosa with Fe^{III}, no Fe^{II}-phen complex was detected, which means that Fe^{III} had not been reduced in this stage. After the protoplast was removed by hot NaOH solution, only a tiny amount of Fe^{II}-phen complex appeared (Figure 3A(b)). The XRD patterns revealed that no distinct diffraction peaks were observed (Figure 3B(b)). According to Majzlan and co-workers[17], the amorphous ferrihydrite is the main form of iron under such condition. When the temperature was raised to 170° C, a certain amount of Fe^{II}-phen complex were found (Figure 3A(c)). And two main characteristic peaks of magnetite at the position of 35.4 (311) and 65.6 (440) appeared (Figure 3B(c)). The broad diffraction peaks suggests that the crystallinity of the sample is poor. The amount of Fe^{II}-phen complex significantly increased and several new diffraction peaks were present and all the peaks matched well with magnetite (Table S1, Supporting Information) with the increase of temperature from 185 to 200° C (Figure 3A(d) and 3A(e)). The results are consistent with existing reports on the effect of Fe^{II}/Fe^{III} molar ratio on the formation of magnetite[18]. However, without the adding of Chlorella pyrenoidosa, the final products were pure hematite (Figure S3, Supporting Information), when all the other experimental conditions were kept the same. Therefore, the addition of Chlorella pyrenoidosa is the key factor for the green fabrication of magnetite nanoparticles. It is known that many substances in the native biomaterials have the reduction ability[19], but further studies are needed to identify which substances are responsible for the production of magnetite nanoparticles. The inset pictures in Figure 3B) show that the black RMMCMs (200 °C) were separated from the solution by the magnet within 90 s and re-dispersed quickly with a slight shake once the magnetic field was removed.

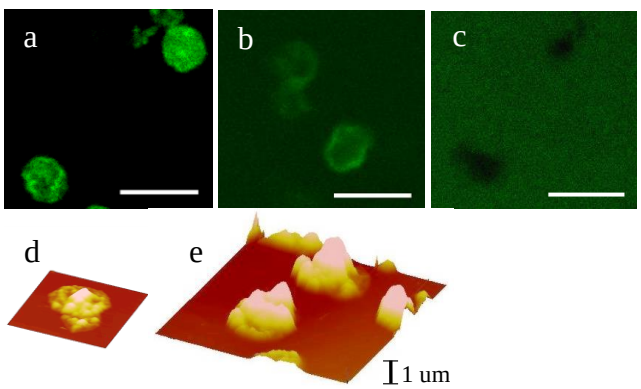

Figure 4. CLSM images of a) auto-loading of FITC-BSA inside the RMMCMs at pH 5; b) and c) release of the encapsulated FITC-BSA from RMMCMs at pH7 and pH9, respectively; d) (5×5 um) and e) (10×10 um) SFM images before and after loading of BSA into the RMMCMs at pH 5. All scale bars are 5 um.

In order to test the potential application of the RMMCMs, bovine serum albumin (BSA) was chosen as a model protein to test its delivery vehicle effect. Confocal laser scanning microscopy (CLSM) was used to obtain the detailed and visible information of the encapsulation and release properties of FITC-BSA (fluorescein isothiocyanate labelled BSA) as a function of pH. At pH 5, after adequate mixing of FITC-BSA and RMMCMs, the fluorescence intensity inside the RMMCMs was much higher than that in the bulk solution (Figure 4a). The scanning force microscopy (SFM) images display the significant difference in the volume of RMMCMs before and after BSA encapsulation (Figure 4d and 4e), which demonstrated that BSA could be auto loaded into the RMMCMs at pH 5 and the protein loading capacity reached to > 600 mg g^{-1}. After the RMMCMs with FITC-BSA were re-dispersed in pH 7 buffer solution, part of FITC-BSA was released from the RMMCMs and diffused into the surrounding solution (Figure 4b). When the pH value was further increased to 9, the interior of the RMMCMs was dark and the fluorescence intensity of the bulk medium was much higher (Figure 4c), which suggests that most of the FITC-BSA is out of the RMMCMs. This can be explained by the electrostatic forces interaction among the FITC-BSA and the multiple magnetite cores within the RMMCMs at different pH values (Figure S4, Supporting Information).

In summary, a novel method was developed to prepare rattle type microspheres with multiple magnetite nano-cores and porous shell. By controlling the hydrothermal synthetic conditions, the cell wall of the Chlorella pyrenoidosa formed the porous biopolymer shell, and the iron precursor (Fe^{III}) was partly reduced and turned into magnetite nanoparticles inside the porous shell with the assistance of Chlorella pyrenoidosa. The multiple magnetite cores not only endow the microspheres with excellent magnetic responsivity, but also play a significant role on the auto loading or release of protein into/out of the RMMCMs under different pH conditions. The method advanced the conventional synthesis methods, which make it possible to supersede harmful chemical reagent with algae protoplast. The RMMCMs may have potential applications including encapsulation of active ingredients, magnetic separation of biological molecules and magnetic drug target delivery.

Acknowledgements

The study was supported by Chinese National Basic Research Program (2010CB933600) and the Science Promotion Program of RCEES, CAS (YSW2013B05). We thank Dr. L. Wang for her help in HRTEM measurement

Notes and references

Department of Environmental Nanomaterials, Research Center for Eco-environmental Sciences, Chinese Academy of Sciences, Beijing 100085, (P. R. China). Fax: (+86)10-6292-3541; Tel: (+86)10-6284-9686; E-mail: gpan@rcees.ac.cn (G.P.)

† Electronic Supplementary Information (ESI) available: Experimental details and relevant figures. See DOI: 10.1039/b000000x/

1 G. L. Li, H. Mohwald, D. Shchukin, *Chem. Soc. Rev*, 2013, **42**, 3628.
2 J. Liu, S. Z. Qiao, J. S. Chen, X. W. Lou, X. G. Xing, G. Q. Lu, *Chem. Commun*, 2011, **47**, 12578.
3 (a) J. Liu, J. R. Cheng, C. Xu, J.M. Liu, Z. Liu, *Appl. Mater. Interfaces*, 2013, **5**, 2503. (b) Y. Ye, L. Kuai, B. J. Geng, Mater. Chem, 2012, 22,

19132. (c) S. H. Hu, Y. Y. Chen, T. C. Liu, T. Tung, H. Liu, D. M. S. Y. Chen, *Chem. Commun*, 2011, **47**, 1776.
4 D. Shchukin, H. Mohwald, *Science*, 2013, **341**, 3458.
5 J. Liu, S. Z. Qiao, Q. H. Hu, G. Q. Lu, *Small*, 2011, **7**, 425.
6 (a) X. Zhang, L. J. Jiang, *Mater. Chem*, 2011, **21**, 10653; (b) Q. Fang, S. Xuan, W. Jiang, X. Gong, *Adv. Funct. Mater*, 2011, **21**, 1902; (c) J. Liu, S. Z. Qiao, S. B. Hartono, G. Q. Lu, *Angew. Chem. Int. Ed*, 2010, **49**, 4981; (d) L. Zhang, S. Z. Qiao, Y. G. Jin, Z. Chen, H. C. Gu, G. Q. Lu, *Adv. Mater*, 2008, **20**, 805; (e) L. Guo, J. Li, L. Zhang, J. Li, Y. Li, C. Yu, J. Shi, M. Ruan, J. J. Feng, *Mater. Chem*, 2008, **18**, 2733.
7 L. Qiang, X. Meng, L. Li, D. Chen, X. Ren, H. Liu, J. Ren, C. Fu, T. Liu, F. Gao, Y. Zhang, F. Tang, *Chem. Commun*, 2013, **49**, 7902.
8 W. M. Zhang, J. S. Hu, Y. G. Guo, S. F. Zheng, L. S. Zhong, W. G. Song, L. J. Wan, *Adv Mater*, 2008, **20**, 1160.
9 D. R. Georgianna, S. P. Mayfield, *Nature*. 2012, **488**, 329.
10 Y. Shi, J. Sheng, F. Yang, Q. Hu, *Food Chem*, 2007, **103**, 101.
11 D. H. Norchtort, K. J. Goulding, *J. Biochem*, 1958, **70**, 391.
12 (a) S. Gao, Y. Shi, S. Zhang, K. Jiang, S. Yang, Z. D. Li, E. T. Muromachi, *J. Phys. Chem*. C, 2008, **112**, 10398; (b) J. R. Chiou, B. H. Lai, K. C. Hsu, D. H. Chen, *J. Hazard. Mater*, 2013, **248**, 394.
13 (a) Z. Schnepp, *Angew Chem. Int. Ed*, 2013, **52**, 1096; (b) Z. Schnepp, W. Yang, M. Antonietti, C. Giordano, *Angew. Chem, Int. Ed*. 2010, **49**, 6564.
14 D. Z. Ni, L. Wang, Y. H. Sun, Z. R. Guan, S. Yang, K. B. Zhou, *Angew. Chem. Int. Ed*, 2010, **49**, 4223.
15 D. Caruntu, G. Caruntu, Y. Chen, C. J. O'Connor, G. Goloverda, V. L. Kolesnichenko, *Chem. Mater*, 2004, **16**, 5527.
16 S. Laurent, D. Forge, M. Port, A. Roch, C. Robic, L. Vander Elst, R. N. Muller, *Chem. Rev*, 2008, **108**, 2064.
17 J. Majzlan, A. Navrotsky, U. Schwertmann, *Geochim. Cosmochim. Acta*, 2004, **68**, 1049.
18 N. Mizutani, T. Iwasaki, S. Watano, T. Yanagida, H. Tanaka, T. Kawai, *Bull. Mater. Sci*, 2008, **31**, 713.
19 R. Shukla, S. K. Nune, N. Chanda, K. Katti, S. Mekapothula, R. R. Kulkarni, W. V. Welshons, R. Kannan, K. V. Katti, *Small*, 2008, **4**, 1425.

Microspheres with multiple magnetite cores, porous shell and high volume fabricated from hydrothermal treated algae cells and single iron source (Fe^{III}).